ELSEVIER

Finite Elements in Analysis and Design 23 (1996) 101–114

FINITE ELEMENTS IN ANALYSIS AND DESIGN

Approximate methods for analyzing the growth of large cracks in fatigue damaged aircraft sheet material and lap joints

Xiangyang Deng, John W. Hutchinson*

Division of Applied Sciences, Harvard University, Pierce Hall, Cambridge MA 02138, USA

Abstract

Several levels of approximation are investigated to account for the effect of small fatigue cracks on the residual strength of aircraft sheet materials and fuselage lap joints containing major cracks. A version of the Dugdale model is proposed which accounts for strain hardening of the sheet in an approximate way and which incorporates a criterion for crack advance leading to crack growth resistance. This model builds upon the model proposed by Nilsson and Hutchinson [1] and accounts for the detailed interaction between the major crack and the small damage cracks. A simpler version of the model uses the damage-reduced local strength of the sheet or joint in assessing the effect of the major crack on residual strength. The simpler approach thus bypasses the necessity of a direct determination of the highly complicated details of the interaction of the small cracks in a lap joint with a major crack.

1. Introduction

There has been considerable effort in the last few years devoted to understanding and analyzing the structural integrity of airplane fuselages in the presence of widespread fatigue damage in the form of small cracks at rivets in the lap joints. Specifically, the issue has focused on whether small crack damage significantly reduces the capability of the fuselage to arrest a major crack produced in an accident scenario. The question is relevant because the original experimental validation of crack arrest design was carried out using test fuselages with undamaged lap joints. The issue is all the more pertinent because a significant fraction of the world aircraft fleet is reaching and exceeding lap joint design life.

Experimental studies of the problem have been undertaken, some of which deal specifically with actual fuselage sections and others which are designed to provide a more fundamental understanding of the interaction of a large crack with small crack damage. In particular, two sets of basic

* Corresponding author. E-mail: hutchinson@husm.harvard.edu.

0168-874X/96/$15.00

experiments have been carried out on flat aircraft sheet material which were designed to provide data on the interaction of a major crack centered in a uniform sheet with small cracks distributed across the ligaments on both sides of the major crack. One set, referred to as the narrow panel tests [2], were conducted on sheets having a width of 20 in. The wide panel tests in the other set had 90 in. wide sheets with central cracks as long as 20 in. [3]. In addition to their value for establishing empirical criteria, the experimental results from the two sets of flat sheet tests have provided a bench mark against which the analysis methods can be assessed.

A number of approaches for analyzing the effect of small crack damage on major crack arrest capability have been proposed. There is general agreement that plasticity plays an important role in the assessment of the effect of small crack damage on major crack arrest in the lap joint of a fuselage. This can be appreciated most directly from the observation that, during mode I tearing of typical aircraft aluminum sheet materials, the plastic zone size extends ahead of a major crack by roughly 2–3 in. while the distance between the small cracks is the rivet spacing, typically about 1 in. Thus, the plastic zone engulfs several damage sites. A general agreement has also emerged from the theoretical studies that small crack damage lying outside the plastic zone has very little effect on the major crack and can safely be neglected in the analysis. A general consensus has not yet emerged as to the complication required in the fracture modeling for analyzing the influence of small crack damage on residual lap joint strength, given a realistic level of accuracy expected for an engineering analysis. Several approaches that involve highly detailed fracture modeling and intensive computer analysis [4, 5] have shown promise for accurate prediction of major/minor crack interaction in uniform sheets. It remains to be seen whether these approaches will prove to be practical when they are applied to the intricacies and uncertainties of the lap joint and to additional complications brought in by the curvature of the fuselage.

The main purposes of this paper are twofold. First, this paper extends Nilsson and Hutchinson's [1] use of the Dugdale model to this class of problems by more realistically accounting for strain hardening and crack growth resistance. Issues related to this and other model which are based on near-tip growth criteria are identified and addressed. The second purpose is to further illustrate the merits of a more simplified approach initiated by Nilsson and Hutchinson [1] for assessing the effect of small crack damage on residual strength in the presence of a major crack. The central idea underlying the simplified approach is that the damage-reduced *local* strength of the sheet or lap joint can be used to modify the fracture analysis without accounting for the fine details of the interaction of the main crack with the small cracks. The determination of the effect of the damage on the local strength of the sheet or joint can be decoupled from the analysis of its role in reducing the residual strength in the presence of a major crack. This suggests a practical approach whereby tests could be employed to measure the effect of fatigue crack damage on lap joint strength, and then that information would be used to carry out the residual strength analysis in the presence of a major crack.

The paper is divided into the following sections. Section 2 introduces two versions of the modified Dugdale model, one which explicitly accounts for the interaction between the main crack and the small cracks and the simplified version which employs the damage-reduced yield strength. The fracture parameters are calibrated for the case of one particular aircraft sheet material. In Section 3, the models are applied to analyze the effect of one or more small cracks ahead of the tip of a long crack in an infinite sheet. In Section 4, the models are used to analyze the narrow panel tests mentioned above. A summary discussion in the final section focuses on one unresolved issue

generic to all models employing near-tip growth criteria and re-emphasizes the potential advantages of the simplified approach.

2. Modified Dugdale models

2.1. Choice of yield stress in Dugdale model for a strain hardening material

The plastic zone in the well-known Dugdale model is represented as a line ahead of the crack tip along which the yielded thin sheet transmits a normal force per unit length $T = h\sigma_Y$, where h is the sheet thickness and σ_Y a measure of the yield stress. When strain hardening can be neglected, σ_Y is taken to be the tensile flow stress, as in Dugdale's original paper. (Strictly speaking, σ_Y should be identified with the plane strain tension flow stress since plastic straining parallel to the crack line is nearly zero. For sheet materials satisfying the Mises yield condition, this results in an increase of the uniaxial flow stress by a factor $2/\sqrt{3}$.) The primary issue to be faced here is the choice of σ_Y when there is appreciable strain hardening, as in the case of the aircraft sheet material analysed later which has an ultimate tensile stress which is almost 50% above its initial yield stress. Since the Dugdale model uses crack solutions for the elastic sheet with an extended crack length on which the plastic zone traction acts, the traction T is the nominal traction with h as the initial thickness of the sheet and σ_Y as a nominal stress (as opposed to a true stress). One suggestion, by Harrison, et al. [6], is to identify σ_Y with the average of the initial tensile yield stress, σ_0, and the ultimate tensile stress (the nominal stress at the necking load), σ_u, i e.

$$\sigma_Y = \tfrac{1}{2}(\sigma_0 + \sigma_u). \tag{2.1}$$

In what follows, we outline an approximate derivation leading to an alternative suggestion, which turns out to differ only slightly from (2.1), as long as the strain hardening is not very high.

For the purposes of this derivation, let δ denote the crack opening displacement in the model, δ_c its critical value at the actual tip, and let J_c denote the associated critical value of the J-integral as evaluated from the elastic crack solution employed in the Dugdale model. As is well known, evaluation of J on a path shrunk down to the Dugdale zone along the crack line gives

$$J = \int_0^R \sigma \frac{\partial \delta}{\partial x}\, dx, \tag{2.2}$$

where σ is the (nominal) stress exerted by the yielded strip and the integration extends from the end of the plastic zone where $\sigma = \sigma_0$ to the crack tip. For the model with the constant flow stress σ_Y, $J = \sigma_Y \delta$ and, in particular,

$$J_c = \sigma_Y \delta_c. \tag{2.3}$$

The value of σ_Y in the derivation below will be chosen to be consistent with (2.2).

Consider a sheet material with a nominal stress-engineering strain curve given by $\sigma(\varepsilon)$ and a true-stress–true-strain curve given by $\sigma_t(\varepsilon_t)$. (Again, strictly speaking, these should be the plane strain tensile curves rather than the uniaxial curves, but this is not the main consideration here.) The sheet material within the zone supplies the traction to the flanks of the elastic Dugdale crack.

Let H denote the thickness of the plastic zone in the plane of the sheet in the direction perpendicular to the crack, and consider it to be approximately constant. In the portion of the zone in which the sheet is necking down, H is approximately the sheet thickness h. Identification of $d\delta$ with $H\,d\varepsilon$ in the integrand in (2.2) gives

$$J_c = H\int_{\varepsilon_0}^{\varepsilon_c} \sigma(\varepsilon)\,d\varepsilon \tag{2.4}$$

for the critical condition, where ε_0 is the strain at initial yield and ε_c denotes the associated engineering strain of the material bridging the tip. Taking the critical opening in the model as $\delta_c = H(\varepsilon_c - \varepsilon_0)$ and equating (2.3) and (2.4), one obtains the desired expression for σ_Y:

$$\sigma_Y = \frac{1}{\varepsilon_c - \varepsilon_0}\int_{\varepsilon_0}^{\varepsilon_c} \sigma(\varepsilon)\,d\varepsilon \tag{2.5}$$

In this paper, the following representation for the tensile curve of true stress versus true strain will be used:

$$\varepsilon_t = \begin{cases} \sigma_t/E & \text{for } \sigma_t < \sigma_0, \\ (\sigma_0/E)(\sigma_t/\sigma_0)^n & \text{for } \sigma_t > \sigma_0. \end{cases} \tag{2.6}$$

If the critical strain in (2.5) is identified with the strain at necking (i.e. corresponding to $\varepsilon_t = 1/n$ in (2.6)), then (2.5) gives

$$\sigma_Y = \frac{n[(n\varepsilon_0 e)^{-(n+1)/n} - 1]}{(n+1)[(n\varepsilon_0 e)^{-1} - 1]}\sigma_0; \tag{2.7}$$

whereas for this same stress–strain curve, (2.1) gives

$$\sigma_Y = \tfrac{1}{2}(1 + (n\varepsilon_0 e)^{-1/n})\sigma_0. \tag{2.8}$$

The dependence of σ_Y/σ_0 on n for each of the above formulas, (2.7) and (2.8) are shown in Fig. 1 for several values of ε_0. As long as the strain hardening exponent is not smaller than about 5, there is little difference between the two results. Since the critical strain will certainly be larger that the strain at necking and since $\sigma(\varepsilon)$ decreases slowly at strains above ε_c, the best choice of σ_Y is likely to be lower than (2.7), perhaps closer to (2.8). In any case, in the present study we will use (2.7) with $n = 8$ which giving a result very close to that obtained by using (2.8).

2.2. *Criteria for crack growth*

Aircraft sheet alloys display crack growth resistance that in some cases can be appreciable. The simplest criterion for crack advance usually used in conjunction with the Dugdale model is the maintainance of a critical crack tip opening displacement δ_c. This criterion does not generate crack growth resistance, but might be justified if δ_c were indentified with the crack opening displacement occuring after an amount of growth relevant to a particular application. A criterion based on the maintainance of a critical crack tip opening angle α_c once the crack has begun to propagate (or, more precisely, a constant near-tip opening profile) does lead to crack growth resistance when it is especially adapted to the Dugdale model, [7, 8]. This criterion has two parameters which can be

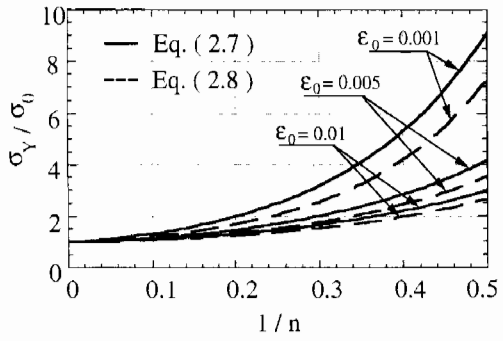

Fig. 1. Dependence of the equivalent yield stress on the strain hardening exponent and initial yield strain.

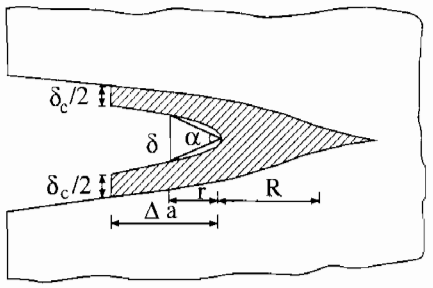

Fig. 2. Crack tip profile of the Dugdale model.

chosen to best fit a given material's resistance curve, one tied to the initial opening displacement and the other to the near-tip opening profile of the propagating crack. The plane stress approach of Newman et al. [4] employs a criterion based on the maintainance of a critical crack tip opening angle, which can be modified in several ways to cope with initiation and the beginning growth stage. The success of this approach has been clearly demonstrated, both in its ability to reproduce test data for aircraft sheet material and in its replication of details of near-tip geometry under growth conditions.

For the propagating crack, define an effective crack tip opening angle by $\alpha = \arctan(\delta/r)$, where, with reference to Fig. 2, δ is the crack opening a distance r behind the current tip. In evaluating δ, one must account for the stretched crack flanks released by the advancing tip. Following Wnuk [8] and Budiansky and Sumner [7], this is done by subtracting from the standard Dugdale opening (at a distance r behind the current tip) the opening experienced when that same material element was severed at the tip. This scheme is indicated in Fig. 2. The criterion for continuing crack advance is $\alpha = \alpha_c$. In the application of the criterion in the present paper, the crack tip is advanced in increments equal to r. Thus, the condition $\alpha = \alpha_c$ can be applied in the first increment following initiation.

A criterion for restarting crack growth must be invoked when the advancing tip breaks through to engulf a small crack. If the small crack were sufficiently long, it is obvious that growth should be restarted with the same criterion used to initiate and grow the main crack, i.e. $\delta = \delta_c$, followed by application of $\alpha = \alpha_c$. It is equally obvious that this restart procedure will not be correct if the small crack is very short, since this procedure gives rise to discontinuous behavior in the limit of a small crack of zero length, whereas the resistance curve behavior should be continuous in this hypothetical limit. Here we propose a criterion which gives continuous behavior for arbitrarily short damage cracks and approaches the behavior expected of a virgin crack for sufficiently long damage cracks. Let L be the length of the engulfed damage crack, and L_T be a transition length parameter. Specifically, with δ_p denoting the value of δ at the instant just before the advancing tip breaks through to the small crack (see Fig. 3), take as the restart criterion:

$$\delta = \begin{cases} \delta_p + (L + L_T)(\delta_c - \delta_p) & \text{for } 0 < L < L_T, \\ \delta_c & \text{for } L > L_T. \end{cases} \tag{2.9}$$

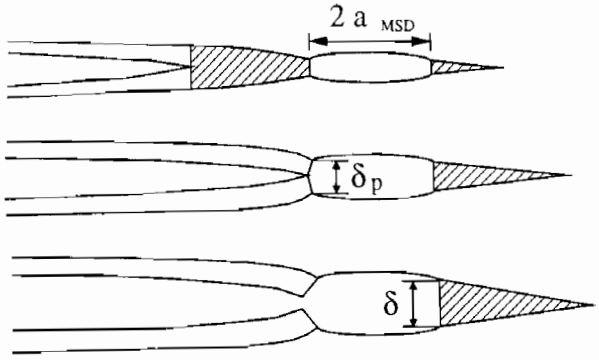

Fig. 3. Simulation of the crack growth and link-up.

The transition length L_T characterizes the size of the small crack such that restarting becomes the same as initiating a virgin crack; it is almost certainly proportional to the small scale yielding plastic zone size. Experiments will be required to establish whether (2.9) is an appropriate restarting criterion and, if so, the value of L_T. Whether (2.9) proves to be valid or not, it seems clear from the discussion above that *some* restart criterion must be invoked for any crack growth model based on a critical value of a quantity such as an opening displacement or an opening angle.

In keeping with the aim of the paper to develop a method which will be applicable to fatigue damaged lap joints, we also consider a simpler approach which does not account for the major/minor crack interaction explicitly. Following Nilsson and Hutchinson [1], we use a damage-reduced yield strength $\bar{\sigma}_Y$ in the Dugdale plastic zone. This idea is motivated by the fact that the plastic zone for the propagating crack extends over at least several damage sites (e.g. rivet spacings) in the actual lap joint problem due to crack growth resistance behavior. For uniform sheets with small cracks of length $2a_{MSD}$ uniformly spaced by a distance l ahead of the main crack tip, the choice

$$\bar{\sigma}_Y = (1 - D_{MSD})\sigma_Y \tag{2.10}$$

reflects the reduced limit strength of a sheet material on either side of the main crack when the damage parameter is $D_{MSD} = 2a_{MSD}/l$. In principle, the choice of $\bar{\sigma}_Y$ for the lap joint could be determined by analysis. However, because of the complications and uncertainities inherent in the joint, it may be preferable to determine $\bar{\sigma}_Y$ by strength tests on fatigue damaged lap joint coupons. Indeed, the justification for a simplified approach such as this over a more detailed one rests on the fact that important quantities influencing lap joint fracture, such as the residual rivet clamping force and friction forces between lapped sheets, are not well characterized yet almost certainly have a significant effect on the joint strength.

2.3. *Calibration for 2024-T3 Alclad aluminum*

The tensile true stress–strain curve for 2024-T3 Alclad aluminum sheet alloy taken from Newman et al. [4] is shown as solid points in Fig. 4. The solid line curve in this plot is the power-law relation (2.6) with the following material parameters: $\sigma_0 = 41.4$ ksi $= 285.4$ MPa,

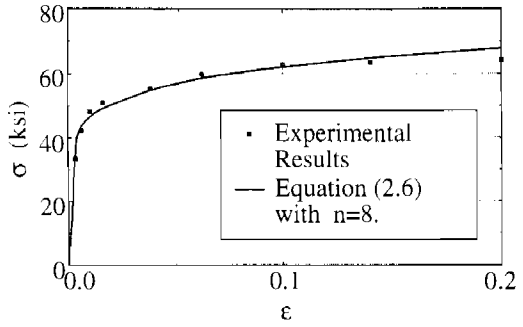

Fig. 4. Stress–strain curve for 2024-T3 Aclad aluminum alloy.

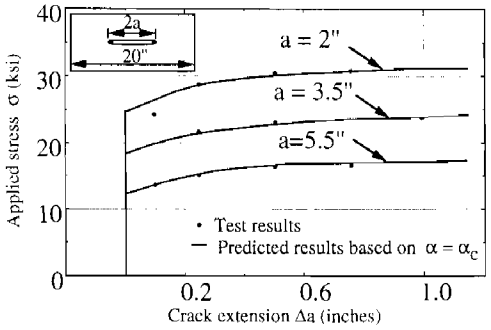

Fig. 5. Comparison of theoretical and test results for narrow panels of 2024-T3 Aclad aluminum alloy with only a central crack. The panel with $a = 3.5$ in. was used to determine α_c.

$E = 10356$ ksi $= 71.4$ GPa and $n = 8$. The effective yield stress for this material to be used in the Dugdale model is found from (2.7) to be $\sigma_Y = 51.3$ ksi. Eq. (2.8) gives $\sigma_Y = 48.9$ ksi..

The solid points in Fig. 5 are experimental data of applied stress versus crack extension for three sheet panels of the 2024-T3 Alclad material [2] with a single central crack. Each of the panels has a total width of 20 in. and the three crack lengths, $2a$, are 4, 7, and 11 in., respectively. The solution to the Dugdale problem for the single central crack in a finite width panel was solved using boundary integral methods. For given choices of δ_c, r and α_c and a given initial crack length, the history of applied stress versus crack length was computed using the first of the criteria discussed above. The value of δ_c can be chosen to reproduce the initiation of growth for a particular experimental record. By systematically repeating the procedure for various combinations of r and α_c, one can arrive at a combination of these parameters which gives a good fit to the growth portion of the record. The middle set of data in Fig. 5 for the 7 in. crack was used for this purpose. The choices are $\delta_c = 9.45 \times 10^{-3}$ in. (corresponding to $K_c = 71$ ksi in.$^{1/2}$ at initiation for small scale yielding), $r = 1$ mm (0.0394 in., which happens to nearly coincide with the sheet thickness) and $\alpha_c = 2.86°$, leading to the middle solid line curve in Fig. 4. The other two solid line curves are the computed results for the panels with initial cracks of 4 and 11 in. in length, and they show good agreement with the corresponding experimental data.

3. Semi-infinite crack interacting with small cracks

To illustrate the application of the CTOA criterion and to highlight important and as well as unimportant factors in the analysis, consider the problem of a long crack in an infinite sheet of the Al 2024-T3 Alclad material interacting with a short crack of length $2a_{MSD}$ such that there is a ligament of length d between them, as shown in the insert of Fig. 6. The main crack is considered to be very long such compared to the size of the plastic zone. In this way, the main crack can be replaced by a semi-infinite crack loaded remotely by the K-field. For the Alclad material, this approximation becomes accurate for main cracks longer than about 15–20 in. In the example

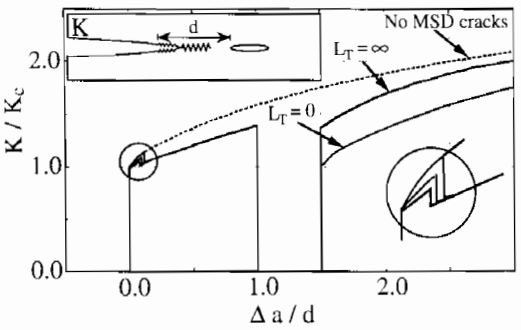

Fig. 6. Effect of small crack interaction with main crack on crack growth resistance in small scale yielding according to several approximations.

shown in Fig. 6, the length of the small crack is $2a_{MSD} = 0.5$ in. and the ligament between the tip of the main crack and the left-hand tip of the small crack is $d = 1$ in.

For reference, the prediction for the sheet in the absence of the small crack is included in Fig. 6 as the dashed-line curve. Let $K(\Delta a)$ denote the applied stress intensity factor after crack advance Δa and let $R = (\pi/8)(K/\sigma_Y)^2$ be associated plastic zone size when $a_{MSD} = 0$. The Dugdale model gives for the stretch-adjusted opening a distance r behind the current crack tip:

$$\delta = \left\{ \frac{8K}{E}\sqrt{\frac{R+r}{2\pi}} - \frac{8\sigma_Y\sqrt{R(R+r)}}{\pi E} - \frac{4\sigma_Y r}{\pi E}\ln[(\sqrt{R+r}-\sqrt{R})^2/r] \right\} - \frac{\bar{K}^2}{E\sigma_Y}, \tag{3.1}$$

where $\bar{K}$ denotes the stress intensity factor when the crack tip was at $\Delta a - r$. The terms in the curly brackets in (3.1) represent the usual opening for the Dugdale model, while the term involving $\bar{K}$ is the stretch-adjustment. The opening angle is $\alpha = \arctan(\delta/r)$, and the condition for continuing growth is $\alpha = \alpha_c$. In applying the criterion, we have advanced the crack tip in increments equal to r. Growth is initiated when δ for the stationary crack (i.e. $\delta = K^2/(E\sigma_Y)$) attains δ_c. For the sheet with $a_{MSD} = 0$, this corresponds to $K = K_c = 71$ ksi in$^{1/2}$.

The three solid line curves in Fig. 6 are for the main crack in the presence of the small crack as calculated using three different modeling approximations for the interaction of the small crack with the main crack which will be discussed below. Apart from the extensions up to $\Delta a/d = 0.15$, the three approximations lead to essentially identical predictions which are indistinguishable in the plot. Thus, we begin by considering the general behavior common to all the approximations. In this example, the crack tip begins to extend just before its plastic zone has spread across the ligament to the small crack. Interaction with the small crack is weak during this brief phase of the loading and the crack growth resistance is only slightly lower than for the case when there is no small crack. The local maximum in K occuring at $\Delta a/d \cong 0.1$ is the point where the ligament becomes fully yielded.

Once the ligament is fully yielded, the plastic zone engulfs the small crack. The basic Dugdale problem associated with this phase of the loading history can also be solved analytically with expressions which are only slightly more complicated than (3.1). The main crack tip extends under increasing K until it reaches the left end of the small crack. The main crack now breaks through and 'jumps' ahead by a distance $\Delta a/d = 0.5$ corresponding to the length of the small crack, as

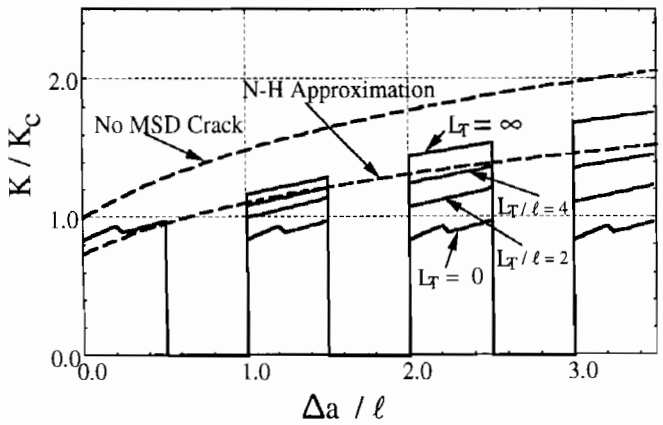

Fig. 7. Effect of small cracks on crack growth resistance in small scale yielding for four choices of the transition length. The approximation based on a damage-reduced yield stress is also shown.

represented by the gap in the history of K versus Δa in Fig. 6. A criterion for restarting crack growth must be invoked. Criterion (2.9) has been used here, it is illustrated in Fig. 6 for the two limits, $L_T = \infty$, or equivalently $\delta = \delta_p$, and $L_T = 0$ such that $\delta = \delta_c$. The limit with $\delta = \delta_c$ is equivalent to restarting the crack as a virgin crack and, therefore, corresponds precisely to a shift of the dashed resistance curve to the right by $\Delta a/d = 1.5$ in Fig. 6. The upper curve, with a restart using $\delta = \delta_p$, should represent the highest resistance curve possible. Thus the two limiting curves shown in Fig. 6 should bracket all possibilities. Since the difference between these curves is not large in this example, predictions for intermediate values of L_T are not given.

The small differences between the curves for crack extensions less than about $\Delta a/d = 0.1$, during the phase of loading in which the plastic zone has not yet engulfed the small crack, correspond to differences in modeling the interaction between the main crack and the small crack. The middle curve accounts for the presence of the small crack but does not include any plastic zone eminating from either of its crack tips. This curve is only slightly below the curve determined for the case where there is no small crack. The lower curve is computed by taking into account the plastic zone eminating from both the main crack tip and from the left tip of the small crack. The effect of the plastic zone of the small crack hardly effects the predictions. The effect of a plastic zone at the right-hand end of the small crack during this phase of the loading should be even smaller and has not been considered. The main conclusion to be drawn is similar to that proposed by Nilsson and Hutchinson [1]: damage cracks not engulfed by the plastic zone of the major crack have little effect on the main crack.

A second example for a very long main crack is given in Fig. 7 for the case of an array of equally spaced damage cracks ($l = 1$ in.) ahead of the main tip, all with the same length, $2a_{MSD} = 0.5$ in. (Note that the tip of the first small crack is now taken to be only 0.5 in. away from the main crack tip, where as in the previous example is was 1 in.) The calculations have been performed using the same values for the fracture parameters as those used in the previous example such that crack growth initiation for the sheet with no small cracks remains at $K_c = 71$ ksi in.$^{1/2}$. The upper dashed curve in Fig. 7 is again the prediction for the sheet with no small cracks (i.e. $a_{MSD} = 0$). The lower

dashed curve is the prediction obtained in precisely the same manner, except that the damage-reduced yield stress $\bar{\sigma}_Y$ given by (2.10) with $D_{MSD} = 0.5$, is used in place of σ_Y. In other words, the lower dashed curve accounts for the small crack damage only through its effect on the yield strength of the sheet. The initiation and growth criteria are based on same values of δ_c and α_c. The four solid curves in Fig. 7 were computed in the same manner as in the previous example – the small cracks are rigorously taken into account in the modeling once they are engulfed by the plastic zone of the main crack, but neglected otherwise. The upper and lower of the four solid curves correspond to $L_T = \infty$ and 0, respectively. The middle two curves were computed with a finite transition length in the restart criterion (2.9): $L_T = 2l$ and $4l$ (i.e. 2 and 4 in.).

For multiple small cracks, the choice of the transition length in the restart criterion has a significant effect on the predictions. Clearly, the simplified approach based on a damage-adjusted yield stress cannot reproduce this effect for arbitrary L_T. Since this example uses material properties and small crack spacings representative of aircraft fuselage applications, it seems prudent to conclude that some further attention should be directed to establishing (or, possibly, dismissing) the need for a restart criterion in any computational model based on near-tip quantities such as those considered here.

4. Central crack with small crack damage

In this section, the modified Dugdale model will be used to analyze the residual strength of the flat sheet panels of 2024-T3 Alclad aluminum with small cracks symmetrically placed on each side of a central major crack. Twelve panels were tested by Broek et al. [2]; three, with a central crack and no small cracks, are considered in Fig. 5. The remaining panels had small cracks as well as the major central crack. The lengths and positions of the cracks for the panels have been published in the papers by Broek [9], Newman et al. [4] and Schijve [10]; the information discussed below is given in Table 1, with the same notation to identify individual tests as has been used by all these authors. The width of all panels is 20 in., the height is 40 in. and the sheet thickness is 0.04 in. The

Table 1
Predicted and test link-up for the specimen P4–P12

Specimen	Predicted first link-up $L_T = 0$ and $L_T = \infty$	Test	Predicted second link-up $L_T = 0$	$L_T = \infty$	Test
P4	23.41	22.50			
P5	17.30	16.88			
P6	15.66	15.00	15.71	17.07	16.50
P7	16.52	16.13	15.21	17.18	15.38
P8	14.93	14.25	16.00	16.93	16.13
P9	21.22	21.00	23.50	25.34	22.13
P10	25.64	25.13	23.75	25.97	25.13
P11	16.13	15.38	16.50	17.85	16.13
P12	28.47	28.13			

values of δ_c and α_c used in the present analysis are those arrived at in Section 2.3 from the panel with the single 7 in. central crack. The results for the panels have been computed using the simplest of the three approximations discussed which ignores the interaction between the major crack and any smaller cracks, as long as the smaller crack is not engulfed by the plastic zone of the major crack. When a small crack is engulfed, it is accounted for exactly in the modified Dugdale model.

First, the panels containing one small crack symmetrically positioned on either side of the major crack will be considered (panels P4, P5, P12). The tests of panels P4 and P12 are similar, and results for P4 are shown in Fig. 8. The applied stress increases monotonically as the crack advances until the plastic zone of the major crack engulfs the small crack. The applied stress drops slightly at this point. As the plastic zone spreads across the outer ligament, the applied load increases slightly as the crack advances until it reaches a maximum and then slowly declines as the major tip closes in on the smaller crack and jumps across the small crack. Crack growth is restarted using (2.9), and curves for the same two limits discussed above are displayed in Fig. 8. During this phase, the applied stress again increases slightly as the crack advances. Once the plastic zone reaches the free edge of the panel, the applied stress is simply the current ligament length as a fraction of the total width times the yield stress σ_Y and, thus, drops linearily with the length of the main crack, as shown. Included in Fig. 8 is the test result for the maximum recorded applied stress for panel P4. In this test, the crack became dynamically unstable at that load. For panel P5, the plastic zone size at initiation already engulfs the small crack and the small drop in load seen for panel P4 does not occur. Plots of applied stress versus crack advance for panels P5 and P12 are otherwise similar to that for P4 and will not be shown. The maximum applied stress prediction is included with the corresponding test result for these panels in Table 1.

The other test panels (P6–P11) have either two or three small cracks symmetrically located on each side of the central major crack. These panels have been analyzed by the same approach. Interaction between the major crack and the small cracks is fully accounted for in the solution of the Dugdale model when the plastic zone engulfs any small crack but is ignored otherwise. In a number of these panels, the plastic zone of the major crack engulfs two of the small cracks before

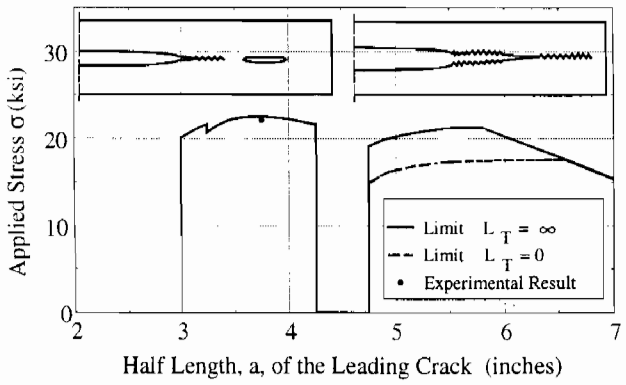

Fig. 8. Applied stress history of narrow panel P4 with one central crack and two small cracks.

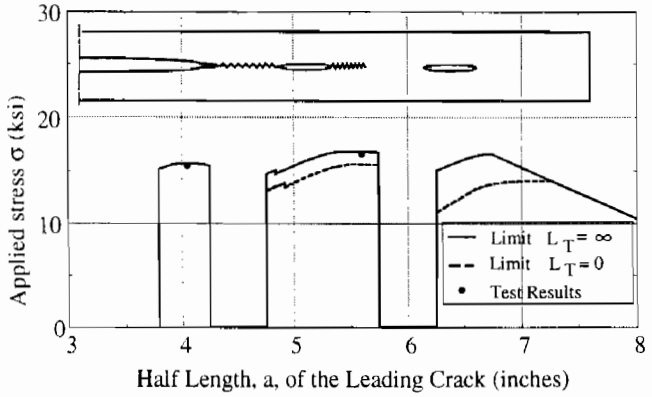

Fig. 9. Applied stress history of narrow panel P6 with one central crack and four small cracks.

the major crack tip breaks through to the first small crack. Results for panel P6, which are representative of the others, are shown in Fig. 9. The first ligament length of P6 specimen is 0.75 in. which is smaller than the plastic zone size when the leading crack begins to grow. Thus, the plastic zone of the leading crack engulfs the first small crack at the beginning of crack growth and the applied load increases and then reaches a local maximum while the plastic zone is still within the second ligament. The test result for P6 for this first maximum is shown. The crack then breaks through the first small crack and is restarted corresponding to the two limits in (2.9) used previously. The plastic zone has not yet engulfed the second small crack. But when the plastic zone reaches the second crack there is a slight drop in the applied stress. Then the applied stress again rises slowly with crack advance until the second local maximum is reached. The test result for this critical stress is closer to the prediction for the restart criterion based $L_T = \infty$ rather than $L_T = 0$, but the difference is relatively small. The results for the two critical stress quantities for the other panels are included in Table 1.

We now apply the simplified approach based on a damage reduced yield stress to panel P6 even though there are only two small cracks on either side of the major crack. The curve shown in Fig. 9 for $L_T = \infty$ is reproduced in Fig. 10, along with the two experimental measurements for that panel. The choice of a sensible damage level D_{MSD} in (2.10) for determining $\bar{\sigma}_Y$ is by no means obvious for this panel because the damage is so nonuniform on either side of the major crack.

With reference to the lengths labelled in the insert in Fig. 10, two extreme choices would be $D_{MSD} = a_1/(l_1 + a_1) = 0.53$ and $D_{MSD} = (a_1 + a_2)/(l_1 + l_2 + l_3 + a_1 + a_2) = 0.16$, based on the net ligament reduction immediate to the tip and on the total ligament reduction, respectively. A sensible intermediate choice is $D_{MSD} = (a_1 + a_2)/(l_1 + l_2 + a_1 + a_2) = 0.41$, based on the two damage cracks and the two adjacent ligaments. The predictions of the simplified approach based on these three choices of D_{MSD} are included in Fig. 10. Apart from underestimating the resistance in the early stage of growth, the choice $D_{MSD} = 0.41$ gives the most reasonable reproduction of the more detailed model and the test points. The wide latitude in possible choice of D_{MSD} for the narrow panel tests is a reflection of the fact that these tests do not realistically scale the relative spacing of the major and small cracks of a full size fuselage joint.

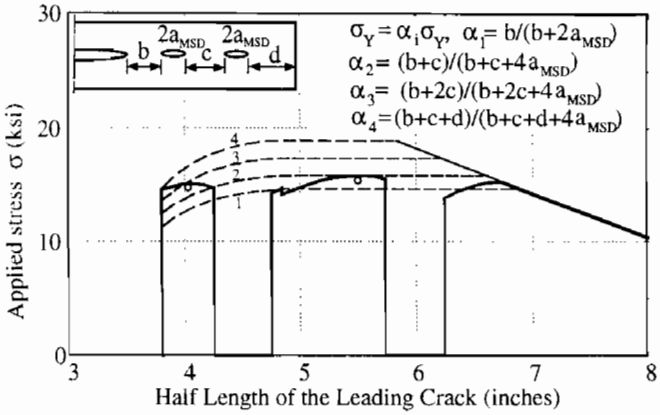

Fig. 10. Applied stress history of narrow panel P6 as predicted by method based on damage-reduced yield strength.

5. Discussion

An approach based on the Dugdale model, modified to account for crack growth resistance, appears to be capable of reproducing the effect of small cracks on the residual strength of a sheets containing a major crack. Moreover, by concentrating the plasticity in the sheet along a predeterminded line, Dugdale-type models have significant computational advantages which will carry over to more complex models of full fuselage sections. One issue which has been identified is the problem of 'restarting' the crack tip growth when the major crack has swallowed up a small crack. A restart criterion must be introduced for any model, such as the present, which uses a critical value of some near tip crack quantity such as a crack opening angle as the condition for continuing growth. From the discussion given in the paper, it would appear that some experimental work is needed to identify the characteristic length L_T of small cracks which are sufficiently long such that the newly extended main crack restarts as if it were a virgin crack.

Even if this model, or more detailed ones, are capable of replicating behavior of the panel tests, it is by no means certain that these same models will be effective in predicting the effect of fatigue damage on the residual strength of a lap joint containing a major crack. The complications of the joint may be too difficult for accurate modeling. Any attempt to model joint failure at the same level as for the panel tests will have to contend with residual stresses in both the rivets and sheets, friction and sliding between sheets, local bending effects, and local geometry. To be effective at this level of detail, the models will obviously have to be capable of predicting the strength of a damaged lap joint in the absence of a major crack. This appears to be a fairly formidable problem in it own right, and it is not clear that the models being developed will be capable of providing accurate predictions. It is this logic which highlights the value of the alternative simpler approach which decouples the determination of the strength reduction of the damaged lap joint from its effect on the residual strength in the presence of a major crack. In principle, combined fatigue/strength tests could be performed on lap joint coupons providing the reduced yield strength $\bar{\sigma}_Y$. Then, this damage-reduced strength would be used in the manner indicated in the body of the paper to calculate the residual strength of the fuselage in the presence of a major crack. In this way, the

computational model for residual strength would not have to bring in the fine details of the lap joint itself. As emphasized, this approach makes sense only if the plastic zone ahead of the major crack extends over several damage sites (e.g. rivet spacings), but this is expected to be the case for the aircraft sheet materials at representative intensity levels.

Acknowledgements

This work was supported in part by FAA Grant 92-G-009 and in part by the Division of Applied Sciences, Harvard University.

References

[1] K.-F. Nilsson and J.W. Hutchinson, Interaction between a major crack and small crack damage in aircraft sheet material, *Int. J. Solids Struct.* **31**, pp. 2331–2346, 1994.
[2] D. Broek, D. Thomson and D.Y. Jeong, Residual strength of flat and curved fuselage panels with and without widespread fatigue damage, US Department of Transportation, 1993.
[3] R. deWit, R.J. Fields, L. Mordfin, S.R. Low and D. Harne, Fracture behavior of large-scale thin-sheet aluminum alloy, Report of National Institute of Standards and Technology, Gaithersburg, MD, 1994.
[4] J.C. Newman Jr., D.S. Dawicke, M.A. Sutton and C.A. Bigelow, A fracture criterion for widespread cracking in thin-sheet aluminum alloys, Paper of 17th ICAF Symp., Stockholm, 1993.
[5] J.H. Park, R. Singh, C.R. Pyo and S.N. Atluri, Residual strength of fuselage panels with widespread fatigue damage, in: *Durability and Structural Reliability of Airframes*, EMAS Publications, A.F. Blom (ed.), London, pp. 413–442, 1993.
[6] R.P. Harrison, K. Loosemoore, I. Milne and A.R. Dowling, Assessment of the integrity of structures containing defects, CEGB Report R/H/R6-Rev.2, Central Electricity Generating Board, UK, 1980.
[7] B. Budiansky and E.E. Sumner Jr., On size effects in plane stress crack-growth resistance, in: *Developments in Mechanics*, Vol. 13 (Proc. 19th Midwestern Mechanics Conf., Ohio State University, Columbus, Ohio) 1985.
[8] M.P. Wnuk, *Proc. Int. Conf. Dynamics Fracture Propagation*, Lehigh University, pp. 273–280, 1972.
[9] D. Broek, The effects of multi-site-damage on the arrest capability of aircraft fuselage structures, FractuREsearch TR 9302, 1993.
[10] J. Schijve, Multiple-site damage in aircraft fuselage structures, Faculty of Aerospace Engineering, Report LR-729, Delft, Netherlands, 1993.
[11] H. Tada, P. Paris and G. Irwin, *The Stress Analysis of Cracks Handbook*, Del Reseach, Hellertown, PA, 1985.